Imperial College London

4th International Workshop on Waves, Storm Surges, and Coastal Hazards
Incorporating the 18th International Waves Workshop

Performance of Wave Radar in Extreme and Breaking Waves

Xiwu PANG[1] (PhD Student)

Supervisor: Dr *Marios CHRISTOU* [1]

[1] Civil & Environmental Engineering Department, Imperial College London, South Kensington, London, SW7 2BX, UK.

Performance of Wave Radar in Extreme and Breaking Waves

Fig 1 The Saab Wave Radar Rex (MicroStep-MIS, n.d.).

- Introduction
- Methodology
- Results
- Conclusion

Introduction

Importance of field measurements

- Calibrating hindcast models (e.g., ERA5, GFS and Ocean Weather datasets)
- Understanding wave behaviour (spectra & crest distributions → extreme wave probability)
- Offshore design conditions (e.g., 1-in-100-year event)
- Ship navigation & safety (X-RADAR systems)
- Accurate wave field data affects forecasting, design, and safety in marine environments.

Measurement Techniques & Limitations

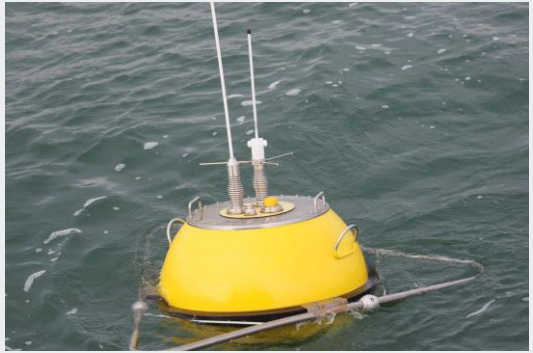

- **Buoys (Moored/Drifting)**
  - Limitations: single-point sampling, discrepancies in wave energy spectra, crest underestimation in extreme seas (Bender et al. 2010, Santamaria et al. 2013, Meylan et al. 2015, Pizzo et al. 2019 and Benetazzo et al. 2025)
- **Laser / LiDAR**
  - Limitations: environmental interference (fog, rain, spray), safety risks, still experimental for LiDAR
- **Wave RADAR (Single Point)**
  - Non-intrusive, safe, high accuracy (mm-level with FMCW), low deployment and maintenance cost, and simple to mount and maintenance
  - Limitations: single-point sampling, underestimates significant wave height & high frequency tail of the spectra in real seas

Motivation

- Gap in Knowledge
  - SAAB radar vs. DWR: underestimation H_s 4–10%, up to 16% in severe sea states (Noreika et al. 2011), underestimates energy spectra $3-5\%$ (Magnusson et al. 2021)
  - Therefore, it is curious what will contribute to the underestimation H_s and the energy spectrum.
  - SAAB radar (theory & lab tests): good agreement with linear random waves (Ewans et al. 2014; Jangir et al. 2022)
  - Environmental challenges: sea spray and droplets → spurious crests, mitigated by QC algorithms (Christou and Ewans 2014; Guy et al. 2024)
  - Furthermore, the wave radar may well be recording breaking waves, but they might be mistaken as erroneous data points in the quality control process.
- Present Study
  - The present study undertakes numerical simulations that replicate the behaviour of a wave radar and examines how it performs in a wide variety of extreme and breaking sea states.

Overview of Wave RADAR Technology

- Devices:
  - Rosemount WaveRadar REX (SAAB), MIROS RangeFinder, RS Aqua WaveRadar REX², Radac WaveGuide 5
- Working Principle:
  - FMCW (Frequency-Modulated Continuous Wave) microwave signal

Radar Model	Range [m]	Sample Rate [Hz]	Measurement Accuracy
Rosemount WaveRadar REX	3–65	up to 10	± 6 mm
RS Aqua WaveRadar REX^2	3–80	up to 10	± 3 mm
Radac WaveGuide 5	2–75	up to 10	± 3 mm
MIROS SM-140/02 RangeFinder	2–23	up to 200	± 5 mm

Methodology

RADAR Mechanism & Wave RADAR Code

- RADAR operates measurement cycle with triangular FMCW sweep
- Assuming FMCW perfectly works in numerical RADAR code
- Original code: MATLAB (Ewans et al. 2014) → adapted to parallel Fortran for efficiency
- Only focus on the Lambertian reflection mode (idealized reflection in all directions)
- Key improvements:
  - Simultaneous scanning of multiple locations
  - Handling multi-valued surfaces in breaking waves

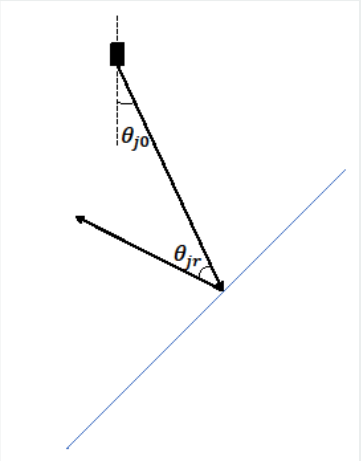

Wave Cases Input

- Input water surfaces:
  - Non-breaking waves: focused wave, second-order Random Wave Theory (SRWT) (efficient, lower cost)
  - Breaking focused waves: simulated with OpenFOAM (waves2Foam toolbox)
  - Breaking + random waves: embedded focused breaking waves at various breaking locations with smooth blending into SRWT surfaces and kept value of the insertion focused wave crest similar to the original wave crest
- Parameters varied:
  - Peak period (T_p), enhancement factor (γ), directional spread (σ)

Results

Second-order Focused Waves

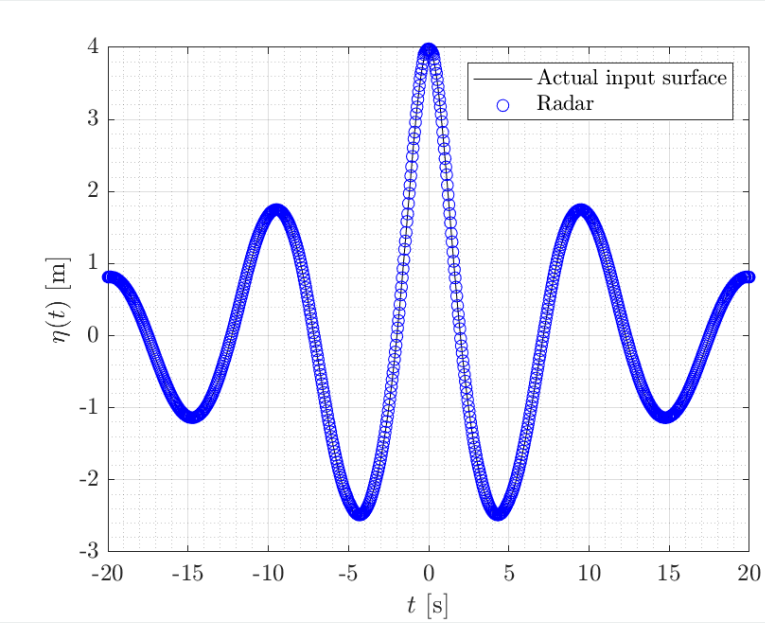

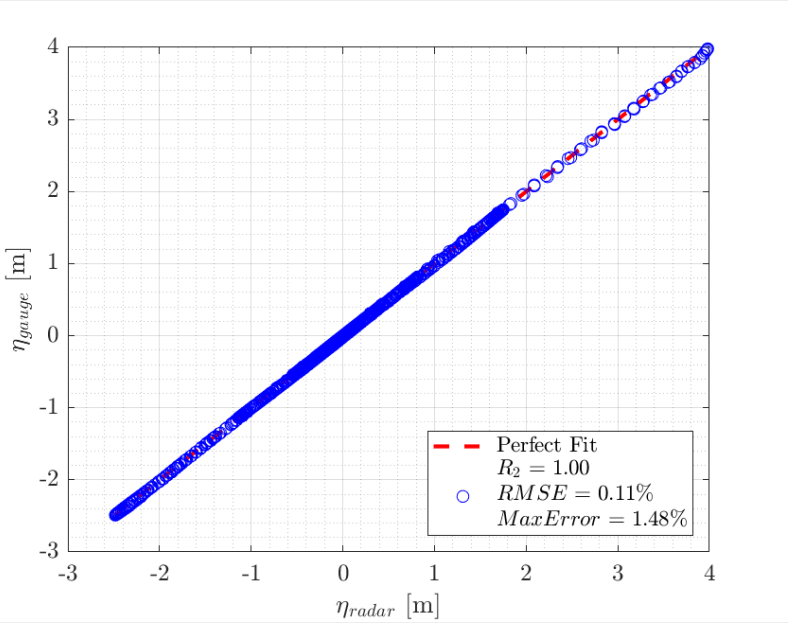

Second-Order Random Wave Theory (SRWT)

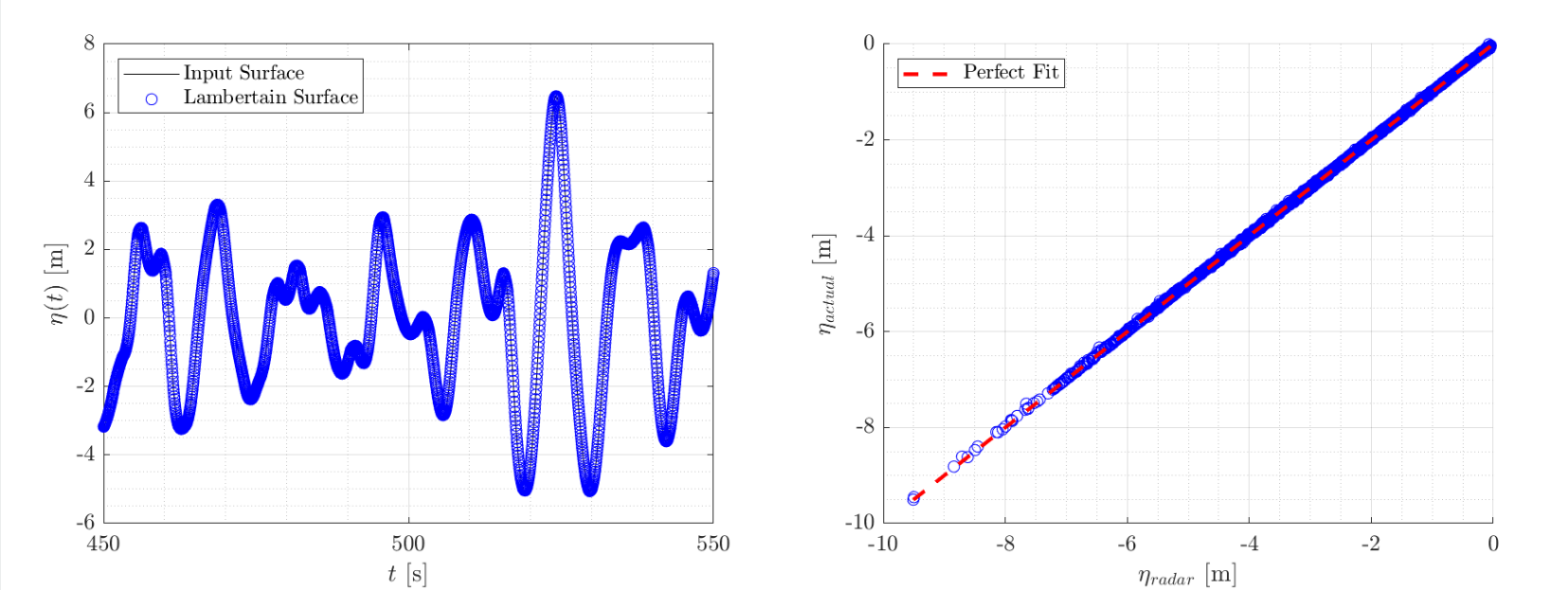

Second-Order Random Wave Theory (SRWT)

RMSE < 0.2% and
Maximum error < 3.1%

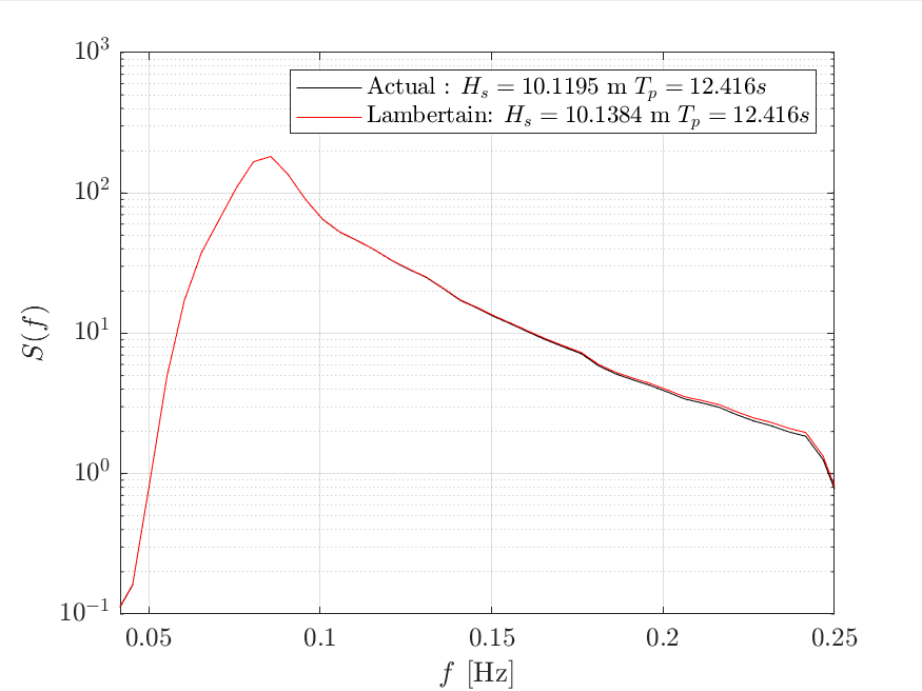

Second-Order Random Wave Theory (SRWT)

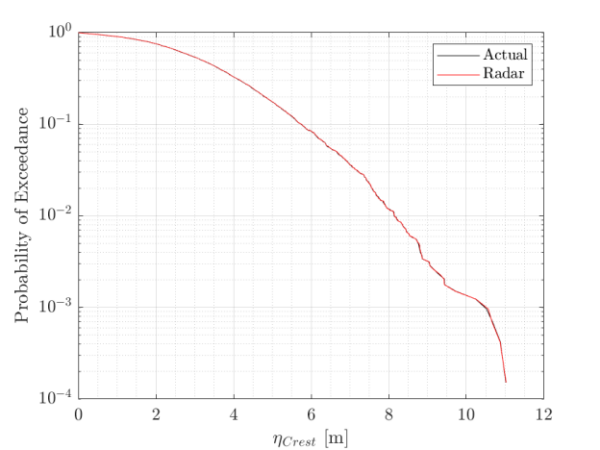

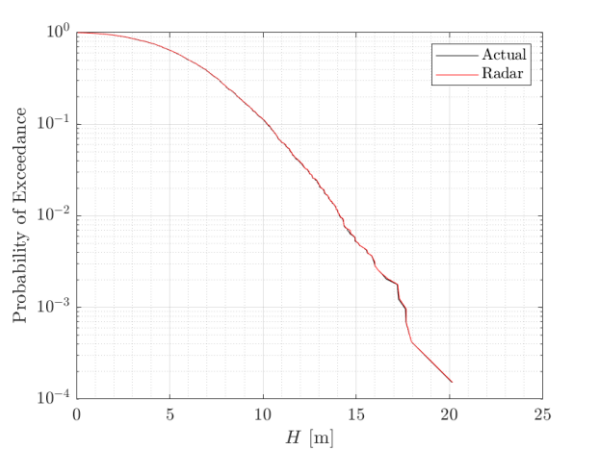

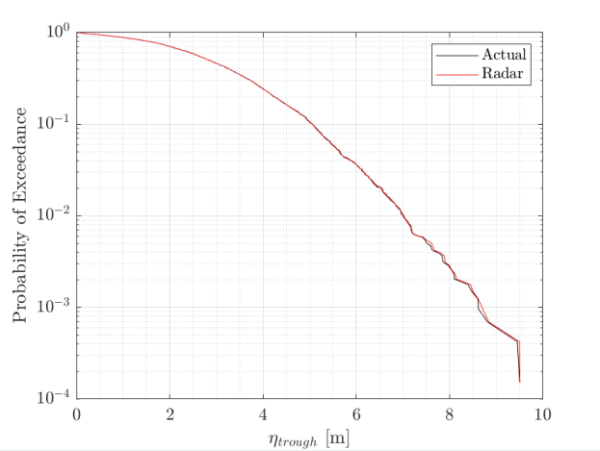

Breaking waves in OpenFOAM

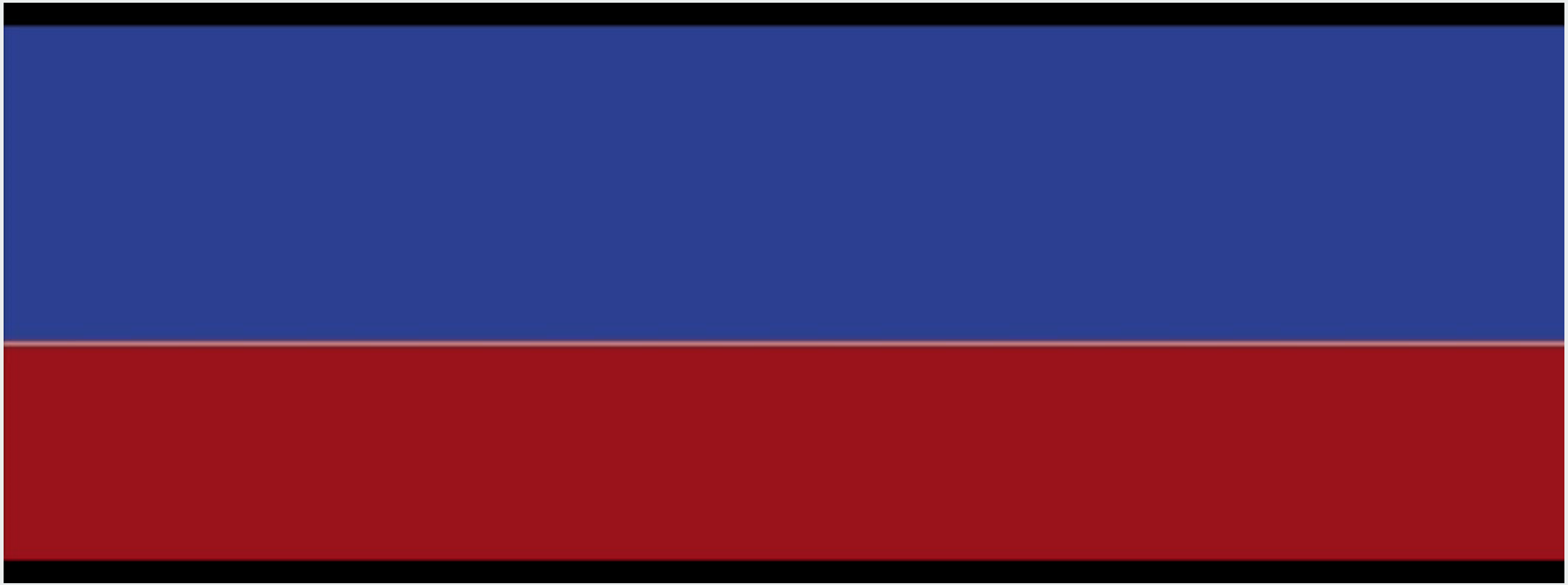

Wave RADAR Code

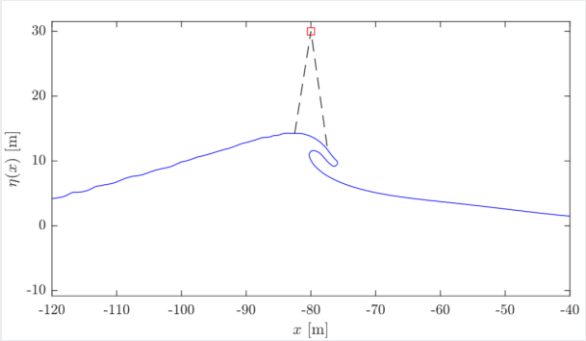

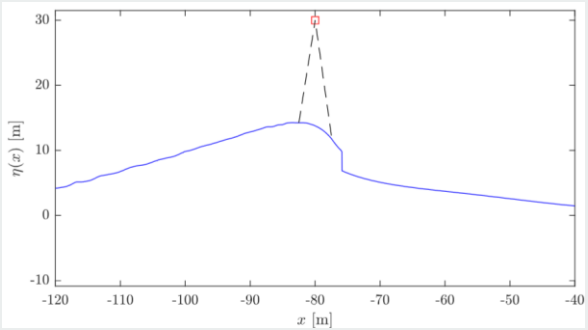

- Pre-processing: Remove “lower surface” in breaking waves (shadow pattern or perpendicular cut)
- According to the equations from Szilard (1982), no echo penetrates the water body.

$$R = \left(\frac{Z_2 - Z_1}{Z_2 + Z_1}\right)^2$$

- where Z is the acoustic impedance, which is taken as: $Z = \rho * c$
- Therefore, only upper surface will reflect the echo

Breaking Focused Waves

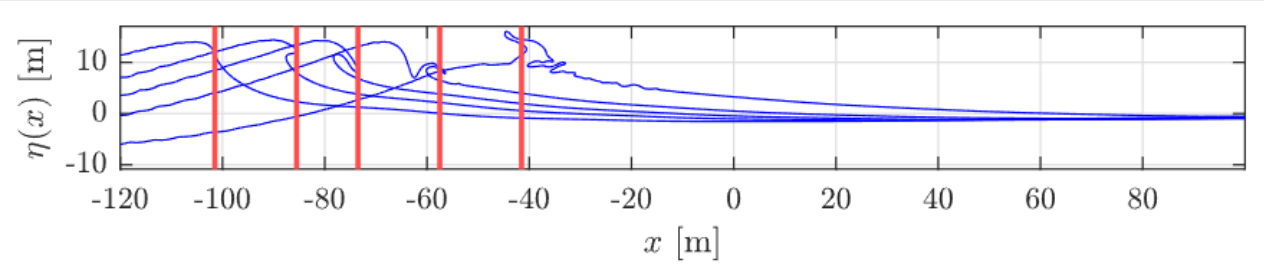

Fig 14: The spatial surface elevation ($\eta(x)$) and wave RADAR location. The red lines from left to right correspond to locations 1 to 5.

Breaking Focused Waves

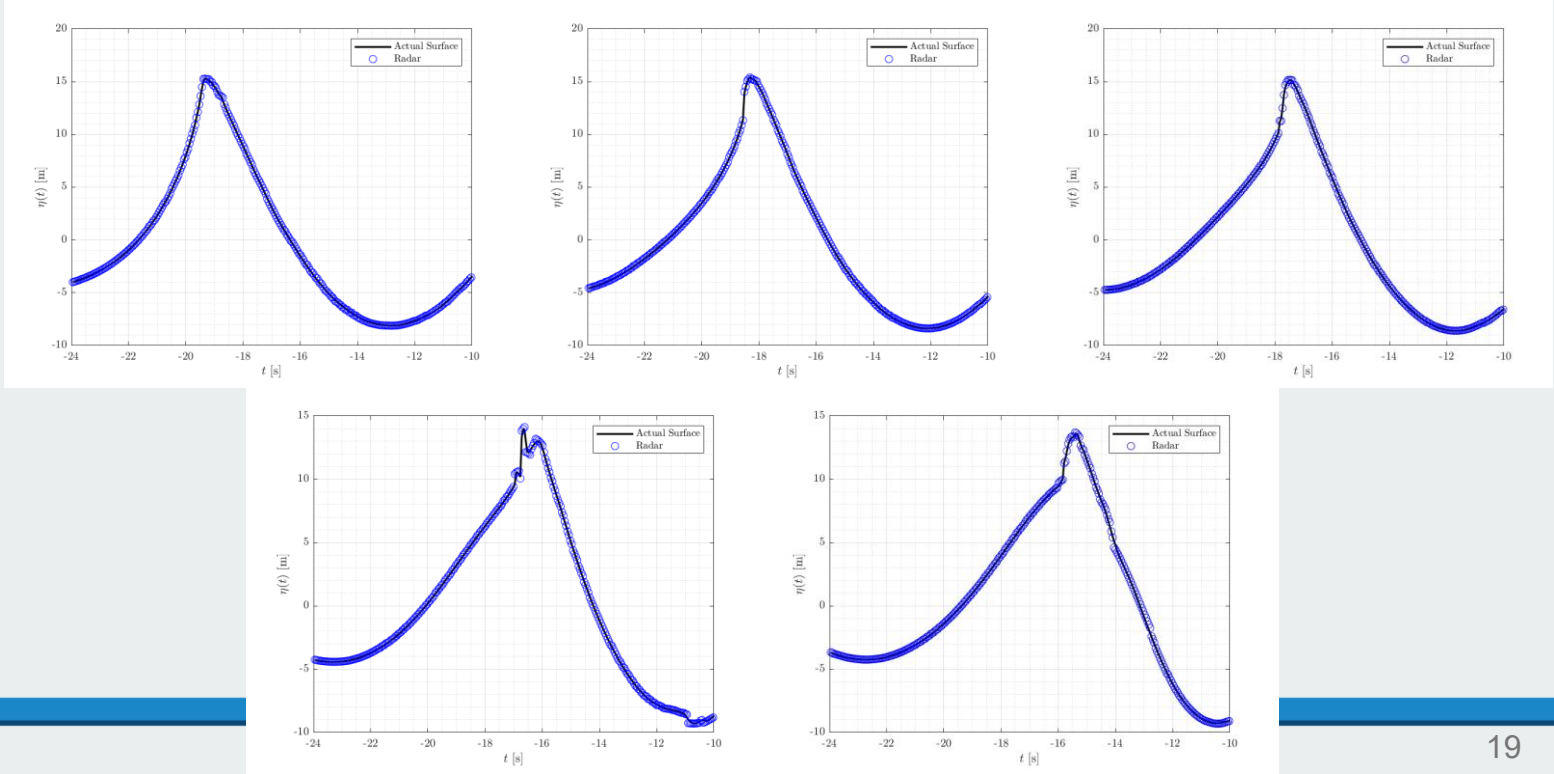

Breaking + Random Waves

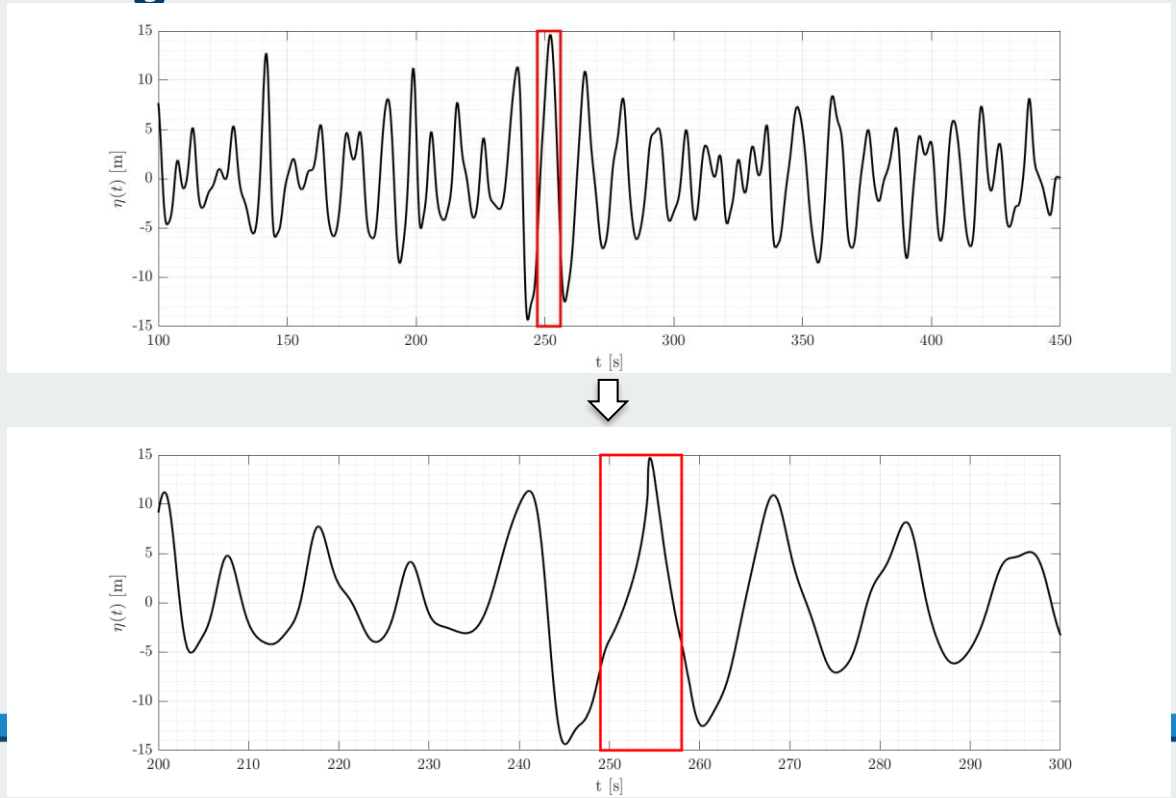

- Breaking focused wave ($\gamma = 2.5$) embedded into SRWT random sea
- Embed the breaking waves from OpenFOAM at five locations

Breaking + Random Waves

Quality Control Flags (Christou and Ewans 2014)
1. Ten consecutive points of equal value
2. Zero up-crossing period > 25s
3. Limit rate of change: S_y
4. Consecutive occurrences of flag 3
5. Crest elevation > 4 standard deviation
6. Consecutive occurrences of flag 5
7. $\mathrm{E}(\mathrm{f} < 0.04\mathrm{Hz}) > 5\%$ total energy
8. $\mathrm{E}(\mathrm{f} > 0.06\mathrm{Hz}) > 5\%$ total energy

Breaking + Random Waves

Effect of Sampling Rate

- Tested $2Hz$, $5Hz$, $10Hz$ (RADAR default)
- Findings:
  - Higher rates ($5 - 10Hz$): accurate surface, capture breaking events
  - Low rate ($2Hz$):Missed breaking crests (sub-sampled profile) produced flatter crests & overestimated Hs (fewer points → larger σ in $\eta(t)$)
  - Energy spectra & wave statistics remain unaffected

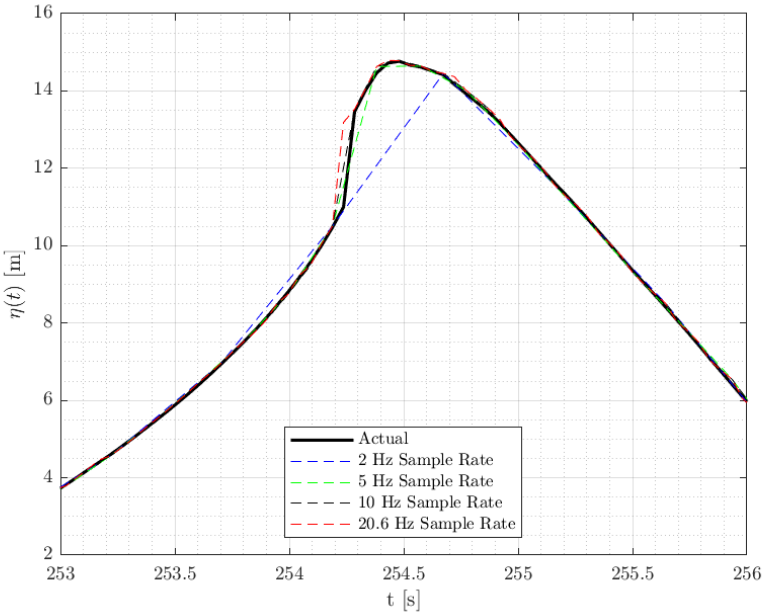

Breaking + Random Waves

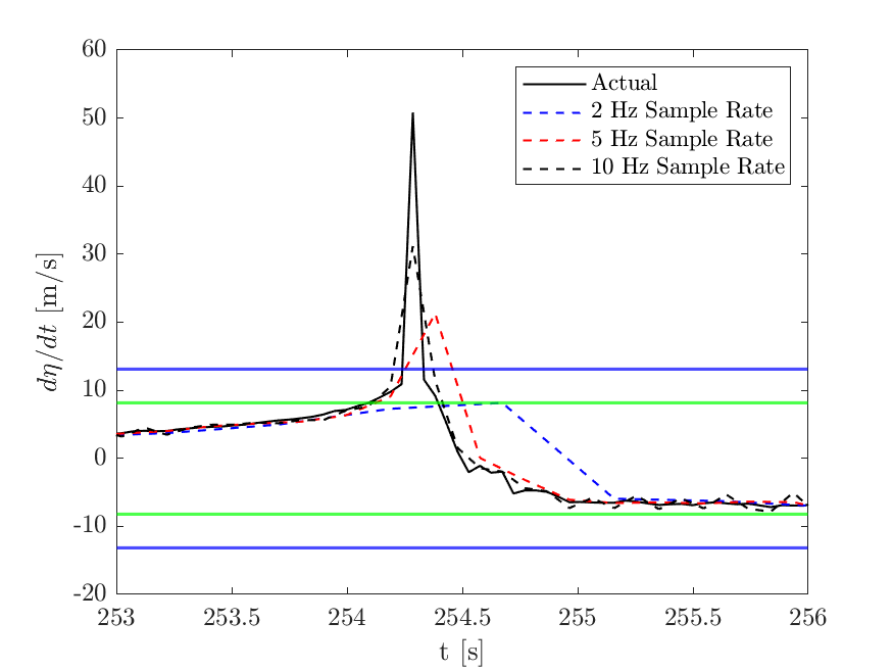

Effect of QC

- Two thresholds tested:
  - Linear limit $S_y = (2\pi\sigma/T_z)\sqrt{2lnN_z}$
  - Second-order limit based on second-order theory

$$S_{y2} = \frac{2\pi\sigma}{T_z}\sqrt{2\ln(N_z)} + \frac{\left(\sigma\sqrt{2\ln(N_z)}\right)^2 k\cosh(kd)}{2,\sinh^3(kd)}\frac{2\pi}{T_z}[2+\cosh(2kd)]$$

where σ denotes the standard deviation, N_z is the number of zero up-crossing periods, $T_z = N/(s_r N_z)$ is the mean zero up-crossing period, N is the number of the data points, and s_r is the sample rate.

Breaking + Random Waves

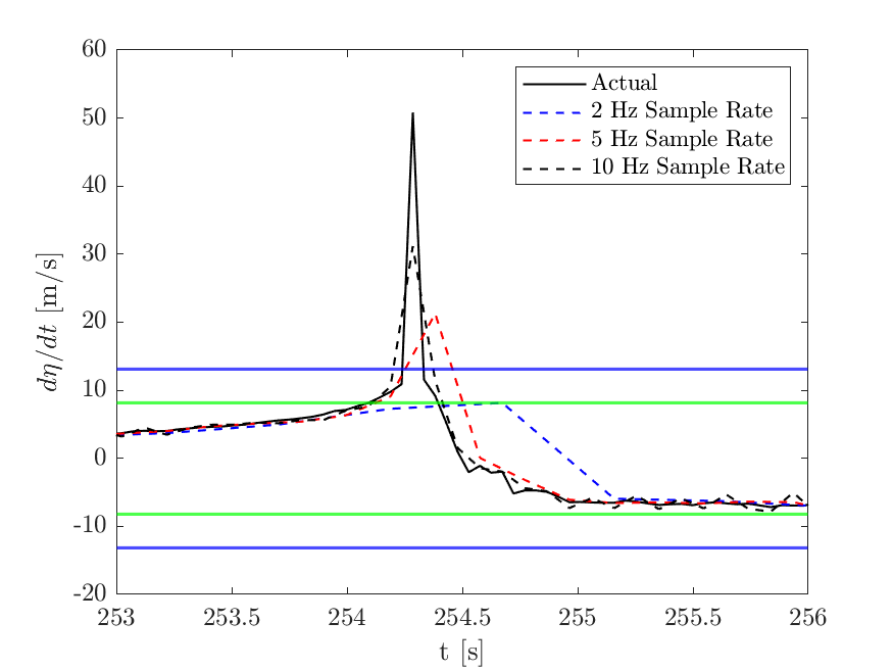

Effect of QC

	Lower sample rate	Higher sample rate
Frequency range	≤ 2Hz (Commonly in old radar system)	≥ 4Hz (Recent radar system adopt)
Effects	Easy to pass the limit rate of change check, but miss the breaking events	Fails to pass the limit rate of change check, but the spikes discarded are likely the breaking events

Conclusion

- Ewans et al. (2014) and Jangir et al. (2022) theoretically investigate RADAR performance under linear wave theory and RADAR works well. The reason of the underestimations in H_s and the higher frequency tail of wave spectra is not found.
- In current study, under second-order wave and fully non-linear breaking wave conditions, theoretical RADAR performance is also good, and the reason of the underestimations is still unclear.
- Theoretically, RADAR reproduces energy spectra, crest/trough stats, significant wave height well in non-breaking sea states under second-order wave theory.
- RADAR captures overturning crests & immediate post-breaking stages.

Conclusion

- Sampling rate & QC effects:
  - Low sampling rates ($\leq 2\mathrm{Hz}$) miss breaking crests, overall elevation trends captured Hs increases with lower sample rate due to higher σ from fewer points and pass the limit rate of change check.
  - Higher sampling rates ($\geq 4\mathrm{Hz}$) capture breaking crests, but fails to pass the limit rate of change check, and QC filters may wrongly remove true breaking spikes.
- Future work:
  - The real operating wave radar are currently testing in the Imperial College London lab (NSTC JIP).
  - The QC issues are needed to be further examined.

Reference

- Christou, Marios and Ewans, Kevin. Field measurements of rogue water waves, 2014.
- Ewans, Kevin; Feld, Graham, and Jonathan, Philip. On wave radar measurement, 2014.
- Pramid, Kumar Jangir; Ewans, Kevin and Young, Ian. On the Functionality of radar and laser ocean wave sensors, 2022.
- MicroStep-MIS (n.d.). Waveradar rex product sheet. https://www.microstep-mis.com. Technical datasheet for WaveRadar REX system. Accessed 2025-07-19.15, 47.
- S. Noreika, M. Beardsley, L. Lodder, S. Brown, D. Duncalf, Com-parison of contemporaneous wave measurements with a rosemount waveradar rex and a data well directional waverider buoy, in: 12thInternational Workshop on Wave Hindcasting and Forecasting &3rd Coastal Hazard Symposium, Kohala Coast, Hawaii, 2011.

Reference

- R. H. Laura A. Fiorentino, W. Krug, Wave measurements from radar tide gauges, Frontiers in Marine Science 6 (2019) 596.
- P. H. T. Guy McCauley, Hugh Wolgamot, J. Orszaghova, Validation of wave radar measurements from the tetra spar demonstrator floating wind turbine, Ocean Engineering 203 (2024)
- A. K. Magnusson, R. Jensen, V. Swail, Spectral shapes and parameters from three different wave sensors, Ocean dynamics 71 (2021)893–909.
- Bender, L., Jr, N. G., Walpert, J., & Howden, S. (2010). A comparison of methods for determining significant wave heights—applied to a 3-m discus buoy during hurricane katrina. Journal of atmospheric and oceanic technology, 27 , 1012–1028.44

Reference

- Santamaria, F., Boffetta, G., Martins Afonso, M., Mazzino, A., Onorato, M., &Pugliese, D. (2013). Stokes drift for inertial particles transported by water waves.Europhysics Letters, 102 (1), 14003.
- Meylan, M. H., Yiew, L. J., Bennetts, L. G., French, B. J., & Thomas, G. A. (2015).Surge motion of an ice floe in waves: comparison of a theoretical and an experimental model. Annals of Glaciology, 56 (69), 155–159. 44
- Pizzo, N., Melville, W. K., & Deike, L. (2019). Lagrangian transport by nonbreaking and breaking deep-water waves at the ocean surface. Journal of Physical Oceanography, 49 (4), 983 – 992.
- Benetazzo, A., Bergamasco, F., Barbariol, F., Ferla, M., Nardone, G., Orasi, A.,Picone, M., Stevanin, A., Marchitiello, A., Pavan, T., Bastianini, M., Pistellato,M., & Cavaleri, L. (2025). Evaluation of the 3d response and performance of and operational wave buoy for coastal wave monitoring. Coastal Engineering, 200 ,104756.

Thanks for listening.

RADAR Mechanism

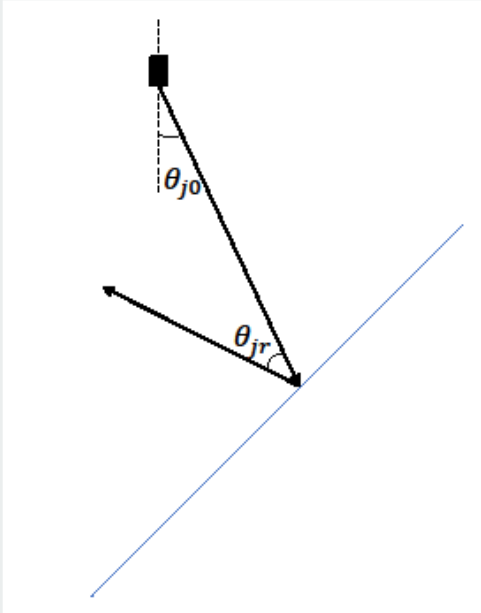

$$\theta_{j0} = \cos^{-1}\left(\frac{x_j \cdot (0,0,z_j)}{x_j|z_j|}\right)$$

$$A_{dB}(r) = -20\log\left(\frac{4\pi 2r}{\lambda}\right)$$

Fig 2: Schematic of wave RADAR simulation where the black box represents the wave RADAR and the blue line is the water surface.

FMCW Mechanism

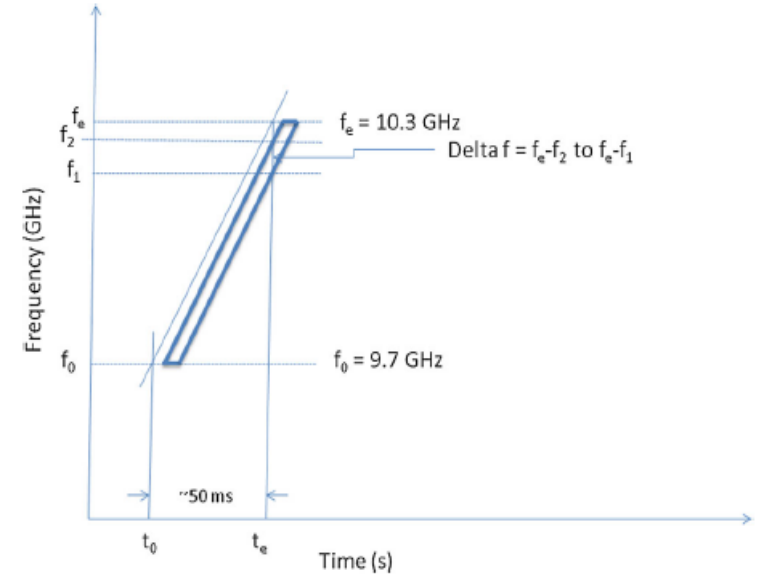

- A chirp cycle spans from start frequency f_0 to stop frequency f_e, with bandwidth $f_B = f_e - f_0$ and duration $T = t_e - t_0$.
- The beat frequency ($\Delta f = f_e - f_1$) arises from the difference between transmitted and received signals.
- The range to target is computed as:

$$R = \frac{c_0 |\Delta f|}{2\left(\frac{\partial f}{\partial t}\right)}$$

where c_0 is speed of light, $\frac{\partial f}{\partial t}$ is chirp slope.

FMCW Mechanism

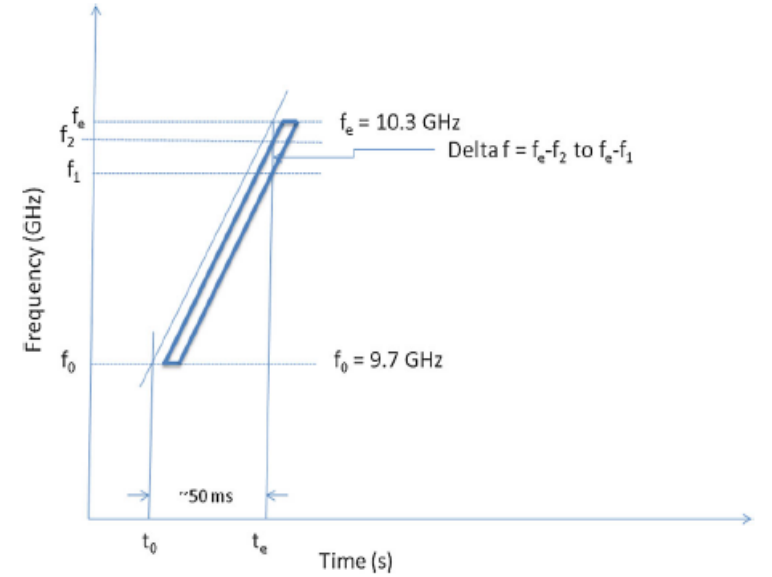

- Each chirp produces N beat frequency samples → digitised → processed with FFT → yields range spectrum.
- Target range is identified from the peak of the range spectrum.

Breaking + Random Waves

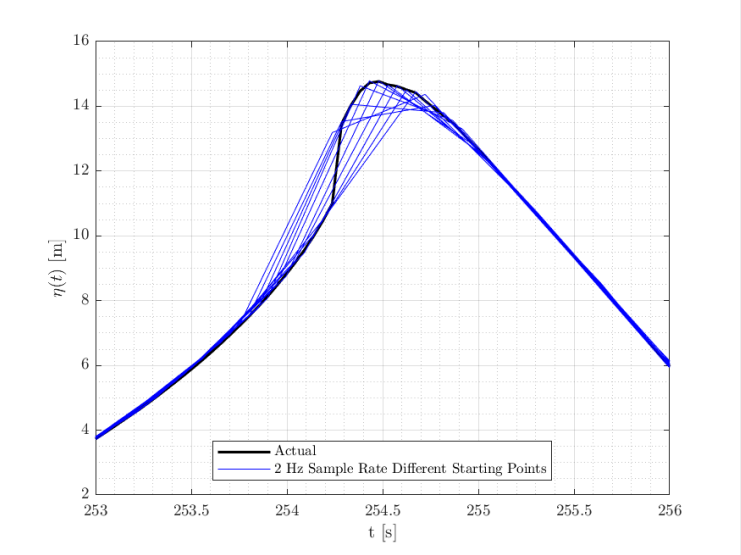

Effect of Start Points

- Different $2Hz$ start times → varied crest shapes
- All missed breaking crests → less steep, phase-shifted profiles

RADAR Mechanism

Lambertian

- Idealized reflection
- Signal scattered **equally in all directions**
- Independent of reflection angle

$$R(\theta_{\mathrm{jr}}) = 1$$

Diffuse

- Signal strength decreases with reflection angle
- More realistic than Lambertian

$$R(\theta_{\mathrm{jr}}) = \cos^{50}(\theta_{\mathrm{r}})$$

Specular

- Signal reflected
- Sensitive to reflection angle

$$R(\theta_{\mathrm{jr}}) = \cos^{1000}(\theta_{\mathrm{r}})$$

RADAR Mechanism

- RADAR operates at 20.6 Hz measurement cycle with triangular FMCW sweep
- Assuming FMCW perfectly works in numerical RADAR code
- Beam footprint: limited to ±5° due to antenna beam pattern
- Three reflection schemes modeled: Lambertian, Diffuse, Specular
- Numerical Governing Equation (Ewans et al., 2014):

$$E_j'(x_j, y_j, z_j) = E(\theta_{j0})A(2r_j)R(\theta_{jr})$$

E_j' : received echo at point (x_j, y_j, z_j)

$E(\theta_{j0})$: antenna signal strength

$A(2r_j)$: attenuation with range

$R(\theta_{jr})$: reflection pattern (Lambertian / Diffuse / Specular)

LRWT Random Waves

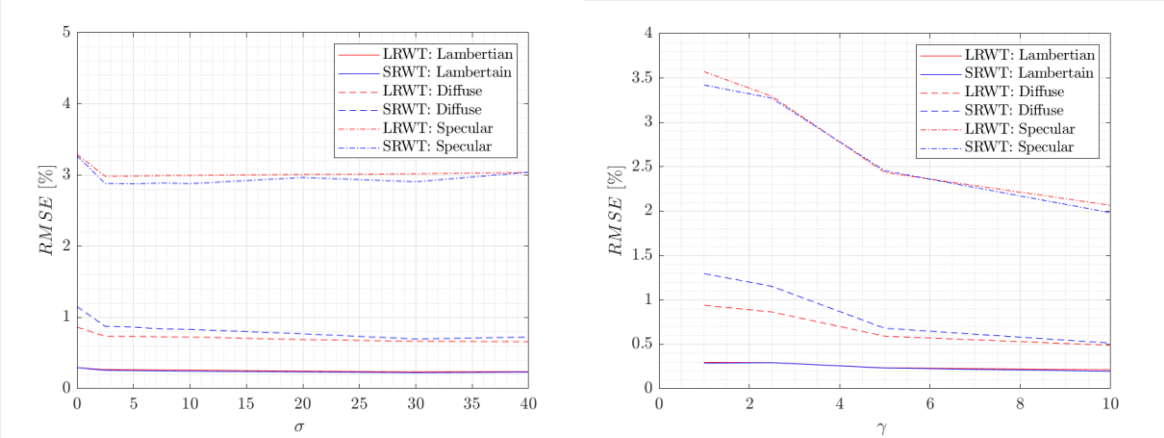

(a) Uni-direction random wave cases (b) Directional random wave cases

Fig 4: The RMSE from the wave RADAR predictions in the random wave cases

- Duration: 30 min simulations
- Accuracy trend: Lambertian > Diffuse > Specular (more sensitive to wave slope)
- RMSE lowest in Lambertian (~0.2%), highest in Specular (~3.5%)

LRWT Random Waves

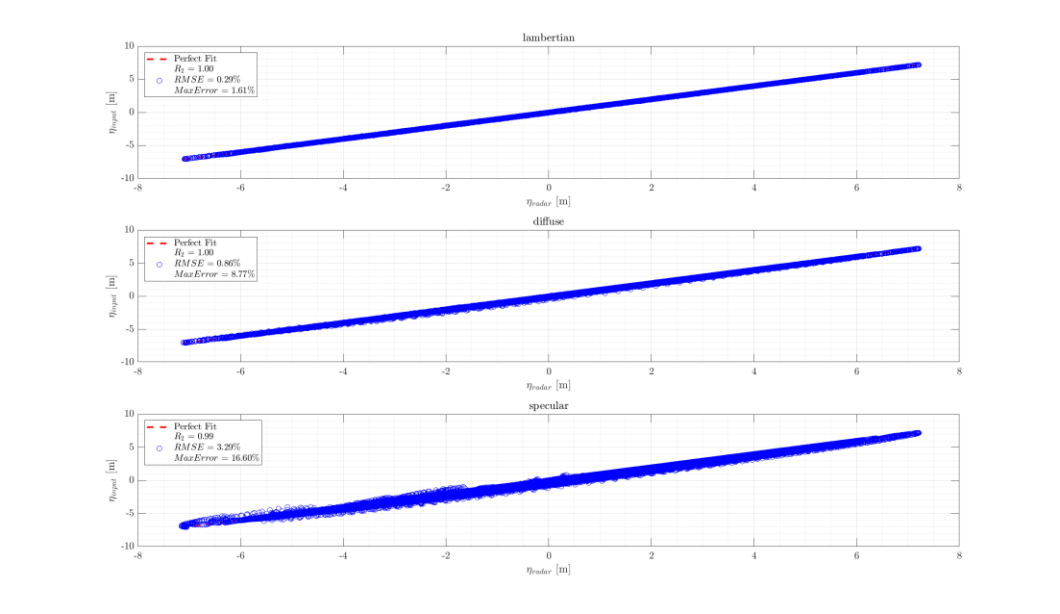

Fig 5: All reflection modes' surface elevation comparison against input surface elevation in scatter plot $\gamma = 2.5$

- Lambertian & Diffuse → good agreement at crests/troughs
- Specular → underestimates troughs

Reflection Angle Effects

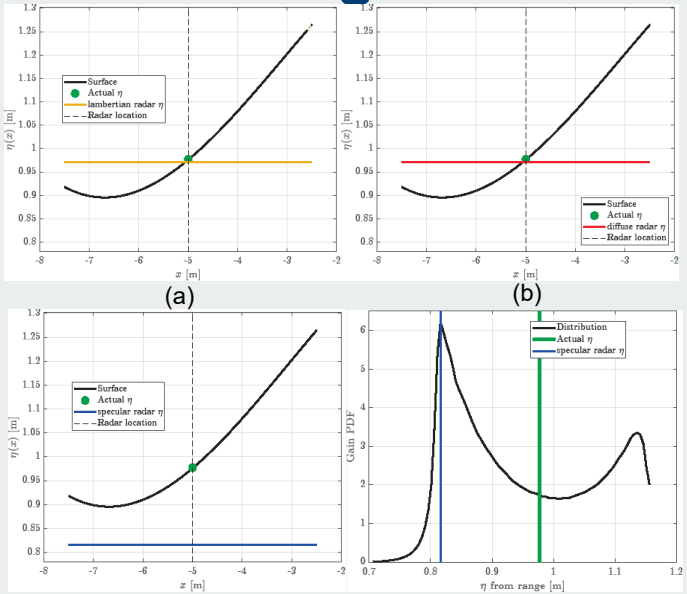

- Specular & Diffuse modes lose signals at steep slopes → underestimation
- 3D footprint effects amplify error (edge reflections)
- Fig 6: Specular produced surface elevations below actual troughs
- Lambertian relatively unaffected by slope

Fig 6: Detailed examination of R1 at $t = 439.09s$. (a), (b) and (c) Spatial surface elevation from LRWT $\eta(x)$ and point-measurement predictions of the wave RADAR at the vertical dashed line using the three different reflection modes. (d) PDF of the gain from the Specular mode.

Second-order Focused Waves

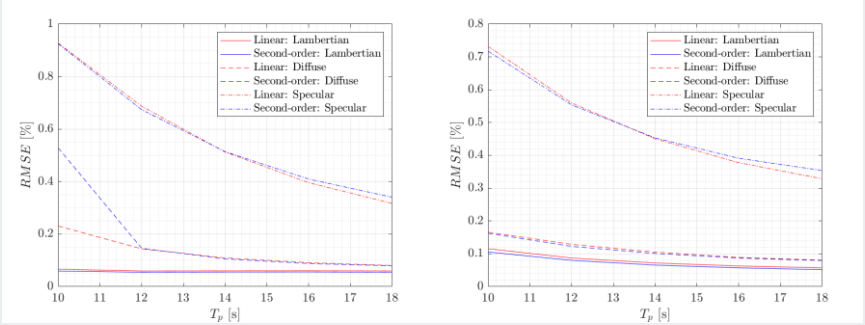

(a) (b)

Fig 7: RMSE plot. (a) $Ak_p = 0.15$ (b) $A_{fixed} = 9$ m.

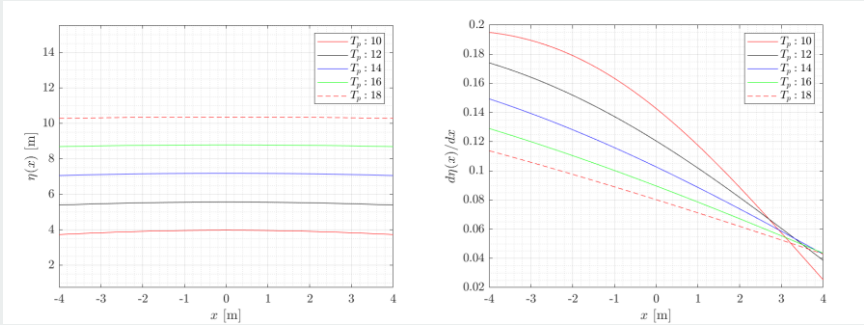

(a) (b)

Fig 8: The surface elevation gradient in the x-domain. (a) $Ak_p = 0.15$ (b) $A_{fixed} = 9$ m.

- Second-order wave theory (SRWT) → steeper crests vs. LRWT
- Effect of T_p (peak period):
  - Longer T_p → gentler slopes → improved RADAR accuracy
  - Shorter T_p → steep slopes → higher maximum errors
- RMSE increases with wave steepness, but remains < 1% for non-breaking cases

Second-order Focused Waves

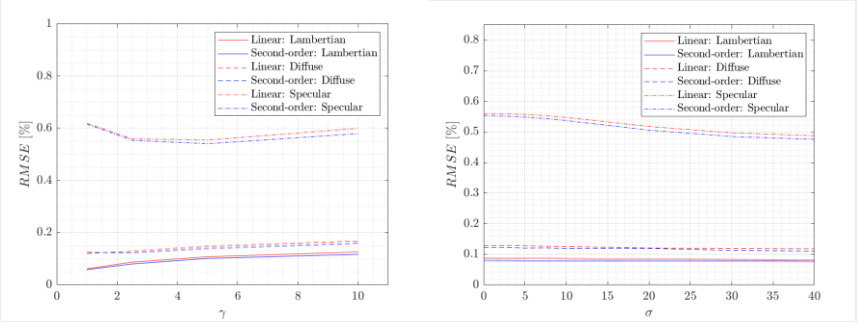

(a) (b)

Fig 9: RMSE plot. (a) Uni-directional focused wave $Ak_p = 0.15$ (b) Directional focused wave $Ak_p = 0.15$ and $\gamma = 2.5$.

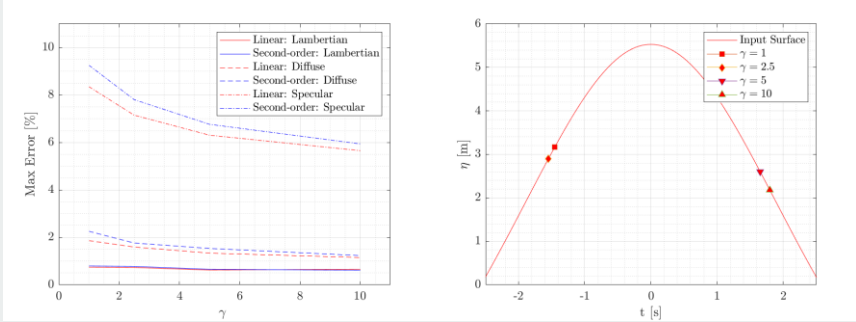

(a) (b)

Fig 10: Uni-directional focused wave $Ak_p = 0.15$. (a) Maximum error plot. (b) The time step corresponding to the maximum error in incident surface elevation (η_t).

- Peak enhancement factor (γ):
  - Larger $\gamma \rightarrow$ increases steepness in surrounding waves $\rightarrow$ more under/overestimation
  - All reflection modes show reduced accuracy at high γ

Second-order Focused Waves

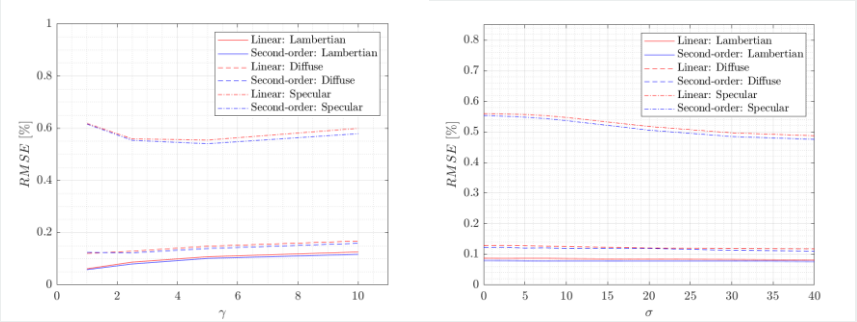

(a) (b)

Fig 9: RMSE plot. (a) Uni-directional focused wave $Ak_p = 0.15$ (b) Directional focused wave $Ak_p = 0.15$ and $\gamma = 2.5$.

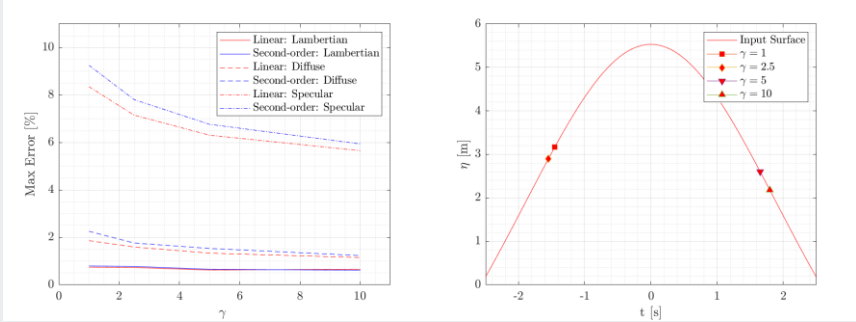

(a) (b)

Fig 10: Uni-directional focused wave $Ak_p = 0.15$. (a) Maximum error plot. (b) The time step corresponding to the maximum error in incident surface elevation (η_t).

- Directional spreading (σ):
  - Wider spreading (σ up to 40°) → reduces steepness → improves performance
  - Lambertian shows little change; Diffuse & Specular benefit most

Directional vs Uni-directional Seas

- Directional spreading improves performance:
  - σ = 40° → Lambertian
- Uni-directional, small γ → poorer results
- Choice of wave theory (LRWT vs SRWT) → little effect on RMSE, but affects max error

Influence of Surface Roughness

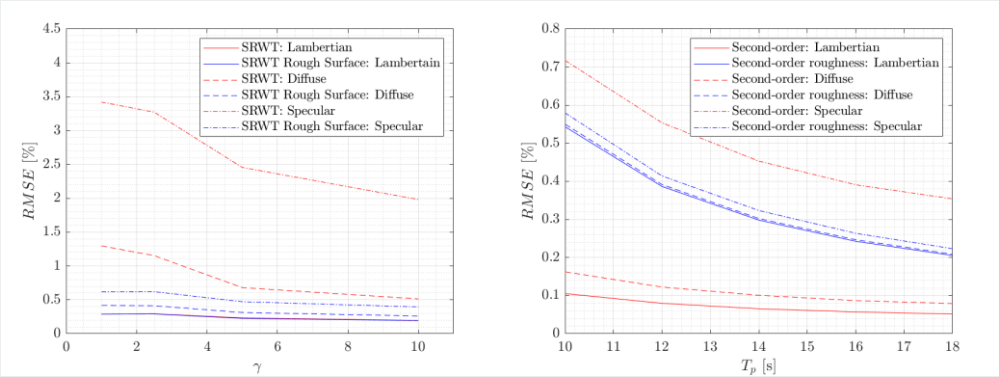

(a) (b)

Fig 13: (a) The RMSE value of random wave cases RG1. (b) The RMSE value of focus wave cases NBG1.

- Adding roughness (α = 0.01 m) improves performance in steep slopes
- Too much roughness ($\alpha \geq 0.16$ m) → distorted profiles
- Roughness helps Specular & Diffuse, little effect on Lambertian
- Suggests real ocean “tiny waves” likely improve RADAR accuracy, therefore, Lambertian is likely is the appropriate reflection mode.

Breaking Focused Waves

- RADAR captures overturning crest & post-breaking moments
- Good crest height prediction, but performance degrades downstream
- Spikes in $\eta(t)$ align with breaking $\rightarrow$ may explain spikes in field data
- Overestimation & underestimation related to ray transport scheme

Influence of Surface Roughness

- All focus and random wave cases with roughness suggest that Specular and Diffuse modes perform as well as the Lambertian.
- Therefore, the Lambertian mode should be the closest mode to the physical wave radar operating in the ocean.

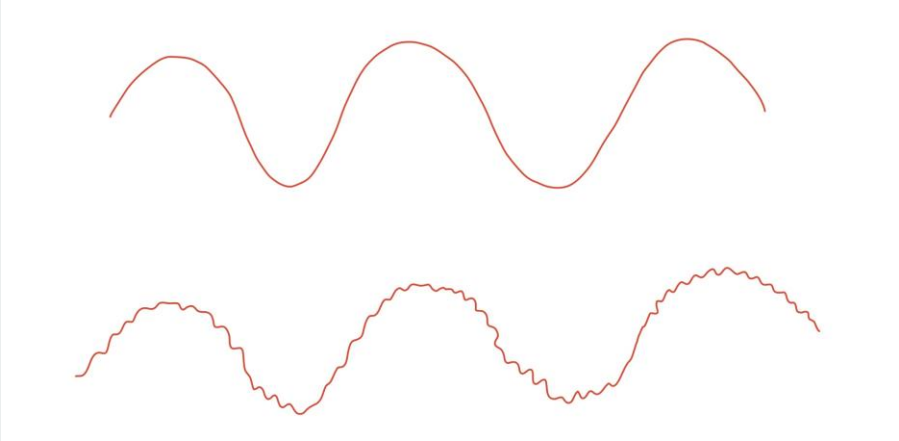

LRWT Random Waves

- Figure 4 illustrates that the surface predicted by Lambertian and Diffuse exhibits better agreement with the actual surface than that from Specular.
- The underestimation of Specular mode is contributed from the effect of reflected angle and the calculation of 3D location.

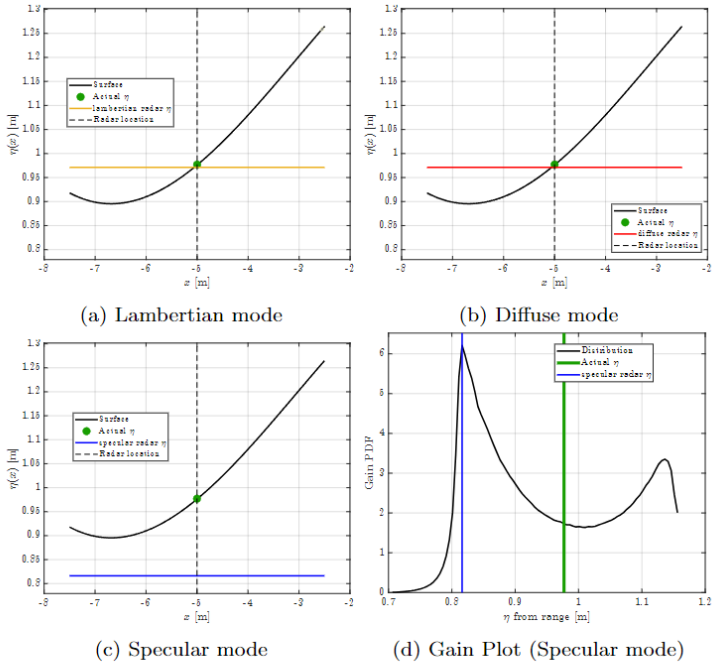

(a) Lambertian mode (b) Diffuse mode

(c) Specular mode (d) Gain Plot (Specular mode)

Figure 4: The actual surface elevation ($\eta(x)$) against the surface from different modes in the scanning area and the Gain Polt from Specular mode at 439.09 s.

SRWT Focus Waves

- Again illustrates that the surface predicted by Lambertian and Diffuse exhibits better agreement with the actual surface than that from Specular.
- The effects of reflected angle and the calculation of 3D location.

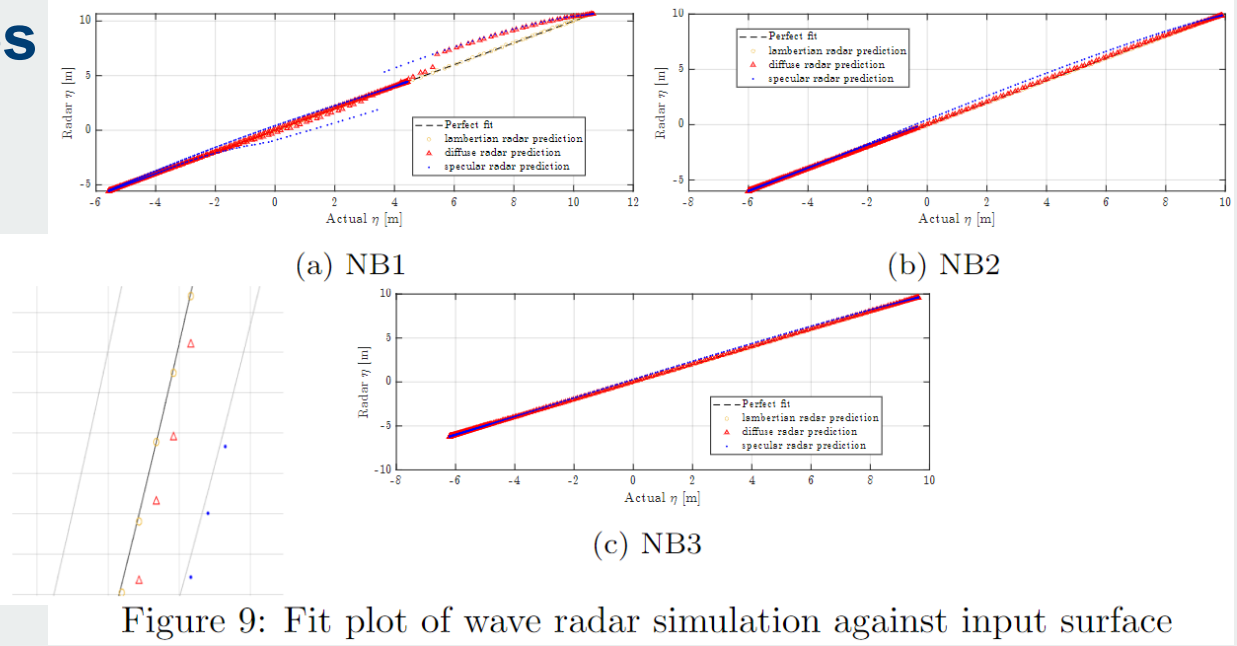

Figure 9: Fit plot of wave radar simulation against input surface

SRWT Random Waves

- In R4, both wave height and wave period show better agreement with the input data compared to R1.
  This implies that wave steepness shifts the water surface in time history.

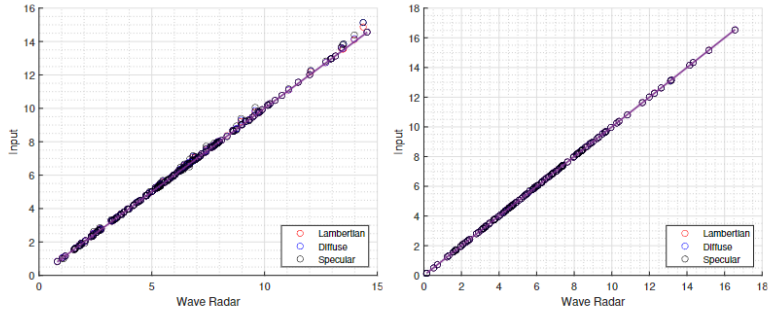

(a) R1 (b) R4

(c) R1 (d) R4

Figure 14: Upper panel is wave height comparison and lower panel is wave period comparison

SRWT Random Waves

- When comparing the RMSE between uni-directional and directional wave cases, different wave radar modes demonstrate good performance in all the directional wave fields with relatively low RMSE.

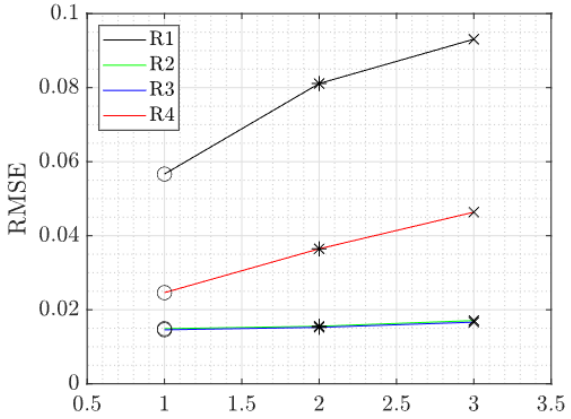

Figure 19: The RMSE value of random wave cases from wave radar. Circle represents the Lambertian mode, start represents the Diffuse mode and cross represents the Specular mode.

Breaking Waves

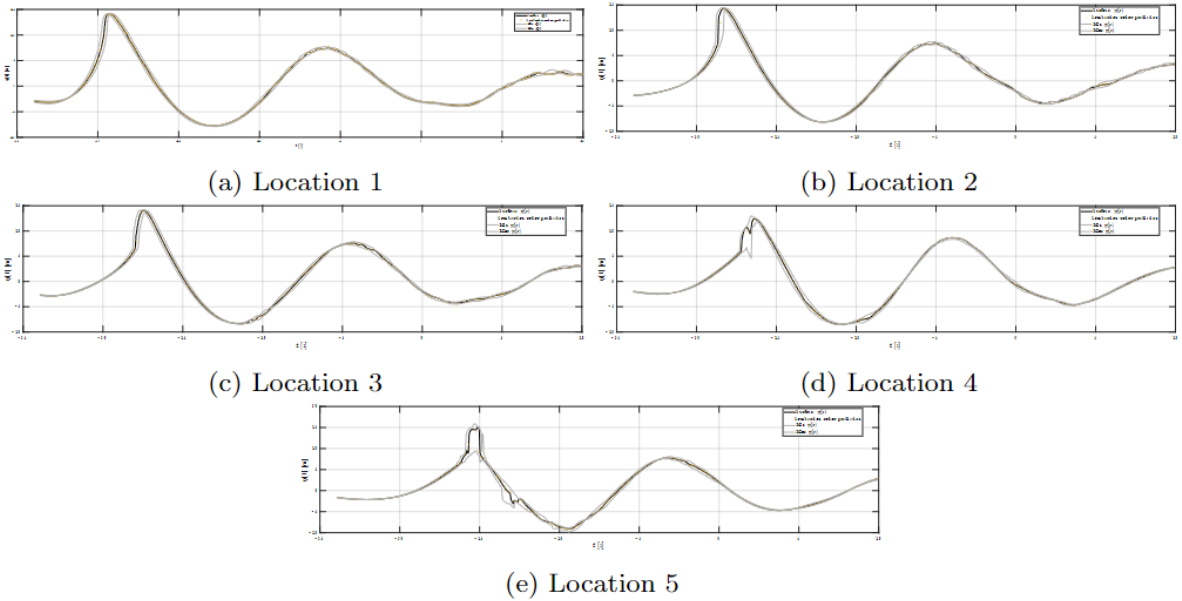

(a) Location 1

(b) Location 2

(c) Location 3

(d) Location 4

(e) Location 5

Figure 22: Transient surface elevation from the original input ($\eta(t)$) comparisons between wave radar simulation and input surface for the breaking wave cases (B1)

Breaking Waves

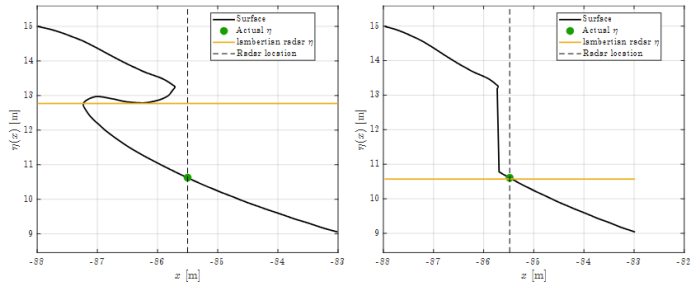

(a) Original input surface (b) Upper input surface

(c) Upper input surface extracted by shadow pattern

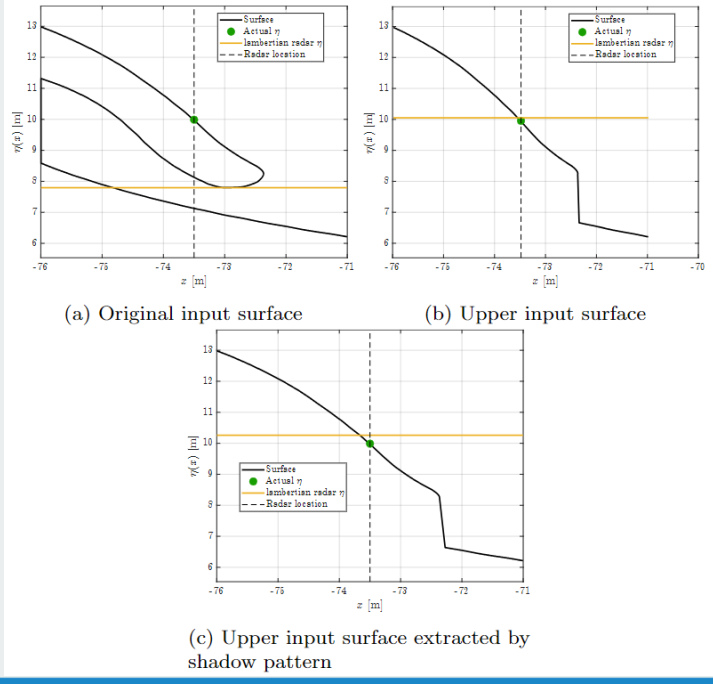

(a) Original input surface (b) Upper input surface

(c) Upper input surface extracted by shadow pattern

Imperial College London

Breaking Waves

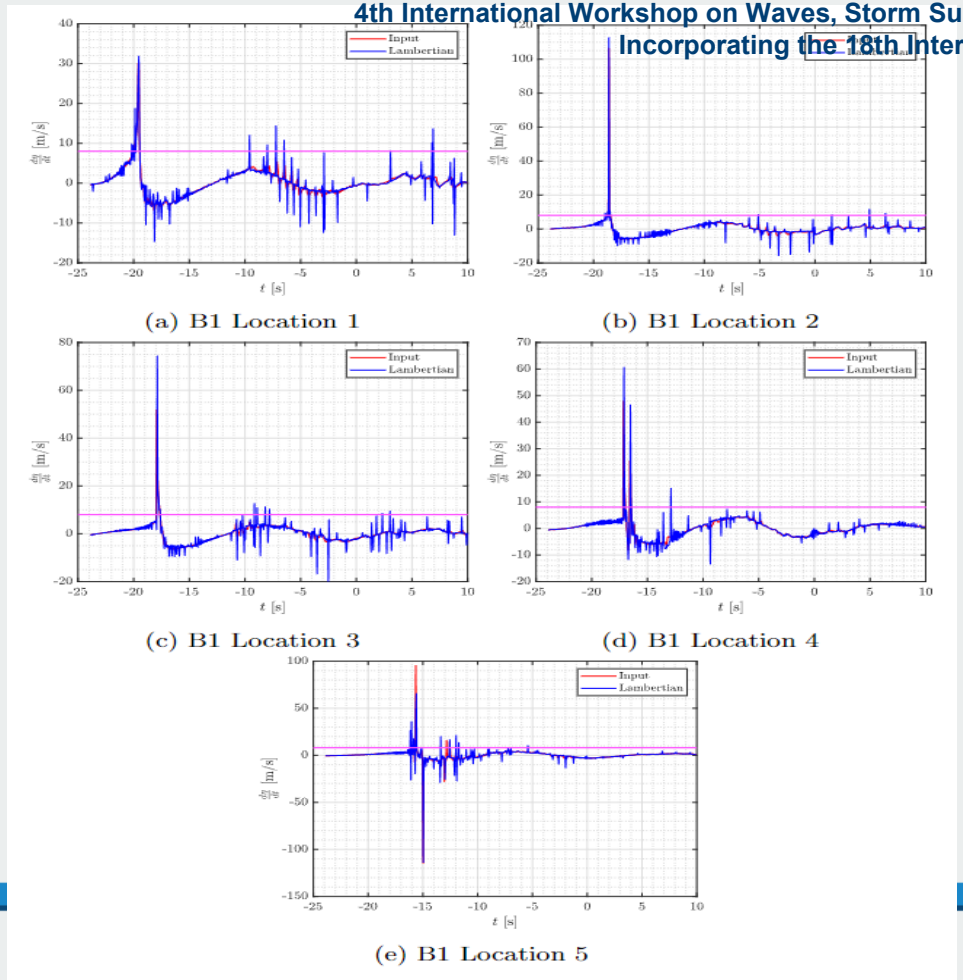

(a) B1 Location 1

(b) B1 Location 2

(c) B1 Location 3

(d) B1 Location 4

(e) B1 Location 5